

PROJECT ADMINISTRATION DATA SHEET☒ ORIGINAL ☐ REVISION NO. \_\_\_\_\_Project No. E-25-M14 (R6191-OA0) GTRC/~~GTX~~ DATE 9 / 4 / 86Project Director: S.S. Bair/W.O. Winer School/~~GTX~~ MESponsor: The Torrington CompanyType Agreement: Research Project Agreement dated 8/11/86Award Period: From 8/11/86 To 5/10/87 (Performance) 5/10/87 (Reports)Sponsor Amount: This Change Total to DateEstimated: \$ 62,871 \$ 62,871 (Fixed Price)Funded: \$ 62,871 \$ 62,871 (Fixed Price)Cost Sharing Amount: \$ None Cost Sharing No: \_\_\_\_\_Title: Needle Bearing InvestigationsADMINISTRATIVE DATAOCA Contact William F. Brown ext. 4820

## 1) Sponsor Technical Contact:

## 2) Sponsor Admin/Contractual Matters:

Mr. Robert Lugosi, Mgr., Product DivisionThe Torrington Company59 Field StreetTorrington, CT 06790Defense Priority Rating: N/A Military Security Classification: Unclass.(or) Company/Industrial Proprietary: N/ARESTRICTIONSSee Attached N/A Supplemental Information Sheet for Additional Requirements.

Travel: Foreign travel must have prior approval – Contact OCA in each case. Domestic travel requires sponsor approval where total will exceed greater of \$500 or 125% of approved proposal budget category.

Equipment: Title vests with SponsorCOMMENTS:See agreement clauses 4 and 5 for publication restrictions on results of research.COPIES TO:SPONSOR'S I. D. NO. 02.219.000.86.R01Project Director  
Research Administrative Network  
Research Property Management  
AccountingProcurement/GTRI Supply Services  
Research Security Services  
Reports Coordinator (OCA)  
Research Communications (2)GTRC  
Library  
Project File  
Other Jones

SPONSORED PROJECT TERMINATION/CLOSEOUT SHEETDate 8/5/87Project No. E-25-M14School/Dept MEIncludes Subproject No.(s) N/AProject Director(s) S.S. Bair/ W.O. WinerGTRC / ~~GTR~~Sponsor The Torrington CompanyTitle Needle Bearing InvestigationsEffective Completion Date: 5/10/87(Performance) 5/10/87

(Reports)

## Grant/Contract Closeout Actions Remaining:

☐

None

☒

Final Invoice or Final Fiscal Report

☐

Closing Documents

☐

Final Report of Inventions

☐

Govt. Property Inventory &amp; Related Certificate

☐

Classified Material Certificate

☐

Other \_\_\_\_\_

Continues Project No. \_\_\_\_\_

Continued by Project No. \_\_\_\_\_

## COPIES TO:

Project Director  
Research Administrative Network  
Research Property Management  
Accounting  
Procurement/GTRI Supply Services  
Research Security Services  
Reports Coordinator (OCA)  
~~Day Services~~

Library

GTRC

~~Research Communication~~

Project File

Other Angela D.

Duane H.

Russ M.

# **NEEDLE BEARING INVESTIGATIONS**

Prepared by

**SCOTT BAIR**  
Senior Research Engineer

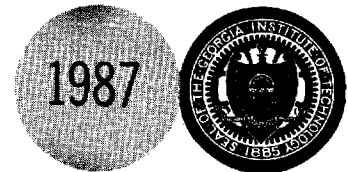
**WARD O. WINER**  
Regents' Professor

Prepared for

**THE TORRINGTON COMPANY**  
59 Field Street  
Torrington, Connecticut 06790

June 1987

**GEORGIA INSTITUTE OF TECHNOLOGY**  
A UNIT OF THE UNIVERSITY SYSTEM OF GEORGIA  
SCHOOL OF MECHANICAL ENGINEERING  
ATLANTA, GEORGIA 30332



**NEEDLE BEARING INVESTIGATIONS**  
Georgia Institute of Technology  
Rheology and Tribology Laboratory  
May 1987

**Abstract**

A Needle Bearing Test Rig has been constructed which allows the measurement of frictional torque, axial thrust, needle axial skew angle, and needle complement velocity for an applied radial load of up to 3500 N and a speed of up to 7000 rpm. Either shaft rotation or cup rotation can be accommodated. Preliminary data indicate that frictional torque is greater for full-complement bearings than caged bearings, that torque is higher for cup rotation than shaft rotation, and that torque is minimized when the needles (full-complement) are axially aligned with the shaft in the load zone. A correlation was found between needle skew angle and axial thrust. Less than one degree change of needle skew is required to go from no thrust to the maximum thrust developed (about 5% of the radial load). Full complement bearings tend to operate with a preferred needle skew direction and attending thrust direction with occasional spontaneous reversals. Operation without thrust and needle skew is not stable. Further research would improve understanding of needle/cage interactions and the effects of geometry changes on needle skew with the possible benefits of reduced torque and increased limiting speed. It is possible to measure the needle/cage contact force in this rig.

**Introduction**

Needle roller bearings are a special case of cylindrical roller bearing in which the roller has a high length to diameter ratio for reduced radial space

requirements. They are used in both the caged and full-complement variations.

Empirical estimates of roller bearing frictional torque have been made (Ref [1,2]) and are frequently used for design purposes. Roller skew is known (Ref [2]) to occur in roller bearings and was measured for a single roller through one revolution of a roller bearing by Nypan (Ref [3]). Axial forces were measured for imposed needle skew angles by Ulezelski et al. (Ref [4]). Needle skew is believed to produce axial force (Ref [4]). A force transducer on the needle bearing shaft of an automotive roller tappet produced the axial force data in Figure 1 using a simulator described in Ref [5]. The axial force is seen to occur at the frequency of needle passage and can be positive or negative with magnitude of as much as 140 N.

A Needle Bearing Test Rig was designed and assembled in the Georgia Tech Tribology and Rheology Laboratory to provide measurements of frictional torque, axial thrust, needle skew angle, and needle complement velocity. Details of the machine design and some preliminary data are reported here.

### Needle Bearing Rig

#### Construction

The Needle Bearing Simulator is shown in Figure 2 in the shaft rotation mode. The cup may also be rotated with the shaft fixed in another mode. The shaft spans three support blocks. The left and center block have identical openings so the drive module and the torque module may be interchanged among them. The center block contains a load diaphragm and load cell for radially loading the test bearing which is always contained in the center block. Regulated gas pressure is supplied to the diaphragm at the top fitting. When the drive module containing the test bearing is in the center block, the cup

rotation mode is available. In Figure 2 the shaft is supported in the right block by a journal bearing. For cup rotation, the journal bearing sleeve is replaced by a special ball bearing which allows both rotation and translation of this right shaft journal. Also at the right block is a ball thrust bearing, thrust cell and micrometer for measurement of the axial force (thrust) applied to the shaft by the needles. The micrometer, pushing through the thrust cell and thrust bearing, preloads the shaft against the drive module (or alternatively, the torque module) at the left block. A flexure on the left end of the shaft increases the axial compliance of the shaft at the left support relative to the axial compliance at the thrust cell end. A preload at the micrometer of 0.076 mm is used for axial force measurements, resulting in 92 N preload on the thrust cell.

The drive module spool is rotated by a 3 mm V-belt, the pulley for which serves as an encoder for a rotational velocity pick-up. Optical probes (Figure 2) of 0.49 mm diameter active element are positioned at the left and right top (load zone) ends of the test bearing by a pair of 3-axis micropositioners (not shown in Figure 2).

#### Torque Transducer

The torque module (Figure 2) provides a housing for the specimen bearing for shaft rotation mode and support for the shaft in cup rotation mode while allowing low friction freedom of rotation of the inner spool. Friction torque may be measured by determining the magnitude of the force required to resist rotation of the inner spool at link "A" in Figure 3. However, it is necessary to correct for the frictional torque of the bearings which support the inner spool. Three configurations were developed to do this.

A four-bearing torque module serves for Configurations I and II. In this module the inner spool is supported by two ball bearings which are housed

inside an intermediate spool which, in turn is supported by two ball bearings. This module is the one pictured in Figure 2 and on the left in Figure 3. Jogging of the intermediate spool causes jogging (oscillating rotation) of the support bearings while the specimen (or the shaft in cup rotation mode) is stationary - Configuration II. If the intermediate spool is fixed and the inner spool is jogged by oscillating the force cell (Figure 3) the same effect is obtained for Configuration I except, of course, that the specimen is not fixed. If support bearing friction is symmetric with respect to rotation direction, jogging causes a noise on the torque signal which if averaged gives the true test bearing torque.

Configuration III is kinematically the same as I. The two bearing torque module is used where the intermediate spool and its two support bearings have been removed to increase stiffness. Only Configuration I or III is appropriate for cup rotation as the friction of the radial and thrust bearings in the right block (Figure 2) must be corrected for. This correction is detailed in a later section.

#### Needle Optical Probes

Two fiber optic probes (MTI Fotonic Sensors) transmit light to and receive reflected light from the trunnions (Figure 4) at both ends of the needles. The 0.9 mm diameter trunnion ends are lapped (600 grit paper) for this purpose. The test bearing cup flanges are machined such that the flange inside diameter is at the needle center line. This way, the flange still axially locates the needles but exposes enough of the trunnions to be optically detected. The needle skew angle changes the phase relationship of the optical probe signals as shown in Figure 4.

#### Data Acquisition Systems

A Gould DASA 9000 Data Acquisition System was used to collect all data when needle angle information was needed. Six channels of data were sampled

concurrently. They included signals from the thrust, load, and torque charge amplifiers, the drive module speed pickup and the two needle optical probes. Sampling rate was 2 to 10 kHz (a rate of up to 300 kHz is available) for 8192 points per channel. Raw data was stored on disc as ASCII files for later reduction.

For measurements not involving the needle optical probes, data was acquired with a Nicolet Storage Scope Model 206 and stored on disc or plotted. Test bearing were not modified for these tests.

### Experimental Procedure

In this work, the measurement of absolute frictional torque is regarded as a quasi-steady state measurement (temperature not necessarily steady) and the thrust and needle angle measurements were handled as transient. For this reason, two test procedures were used. Test bearings were cleaned in acetone in a "sonic" cleaner before being pressed into the torque or drive module.

#### Absolute Friction Measurements

For all absolute friction tests, the inner spool support bearings in the torque module were jogged at a frequency of 1 Hz and an amplitude of  $11^\circ$  for a maximum velocity of 13 rpm. Each test bearing was lubricated once with a 10W-40 commercial engine oil. Oil was added by syringe until it overflowed from the horizontal bearing. The test procedure follows:

- 1) Without load, the bearing was brought to speed and jogging of the torque module begun.
- 2) The load was applied for about five (unless noted) seconds. Averaged data of this period of time yielded the torque level.
- 3) The load was removed and the drive motor braked.



- 4) The drive module was jogged by hand several times. Data of this period of time were averaged to give the zero friction level.
- 5) Voltage levels from data averaged during (4) were subtracted from those averaged during (2) to give absolute frictional torque.

The thrust signal level was found to be sensitive to normal load, possibly due to deflection of the shaft which would shorten its effective length. For this reason, the thrust signals that were recorded during these tests are not reported as the zero thrust signal level is not known. However, any transients in thrust which occurred are stored on disc.

Friction and thrust data were recorded on the Nicolet oscilloscope. Friction data was graphically averaged on this device which gives a digital reading of voltage levels. If the inner spool support bearing friction is symmetric, averaging data while jogging these bearings removes this source of error.

#### Needle Angle/Thrust Measurements

Needle angle/thrust tests were performed in the shaft rotation mode using the two bearing torque module in Configuration III without jogging of the inner spool. A grease (NLGI reference system "A") was chosen for the lubricant for these tests to reduce the possibility of oil drops interfering with the optical path between the probes and the needle ends. At this time it is not felt that oil will be a problem.

Care must be taken to ensure that the optical probe is responding to light reflected from its corresponding needle end and not to light which passes between the needles from the opposite probe which can occur when the probe is positioned close to the shaft. See the probe placement detail in Figure 4. The waveform from one probe should be unaffected when the power to the opposite probe is removed.

The Gould Waveform Recorder was used to sample data with the trigger set for a  $\pm 20\%$  window on the thrust range. Pretrigger is set at 50% so that the trigger event occurs in the center of the data file. Sample rate should provide at least 10 points per needle passage. The test procedure follows:

- 1) Bring the shaft to speed then apply the load.
- 2) Adjust the position of the two optical probes to maximize their signals as viewed on an analog scope.
- 3) Zero the load, thrust, and torque charge amplifiers.
- 4) Arm the recorder. The recorder triggers when the thrust level rises or falls by 20% of the recorder range.
- 5) When the record is complete, brake the motor.
- 6) Jog the drive by hand with normal load still applied and the thrust signal level being sampled by the Nicolet scope.
- 7) Graphically average the thrust signal level during (6) to be supplied as the zero thrust signal level to software later.
- 8) Transfer the 48 k bytes of data to the computer and store on disc.

The data on disc is reduced at a later time by the program SHFTR3.BAS and plotted by the program PLOT3.BAS.

### Test Results

#### Friction Torque Tests

The friction coefficient,  $\mu$ , can be defined as

$$\mu = \frac{T}{r_s W}$$

where T is frictional torque,  $r_s$  is the radius of the shaft and W is the radial load on the bearing. Seven pairs of tests were conducted with shaft

rotation to evaluate the differences between Configuration I and II (Figure 3). On the average, the frictional torque differed by 2.6% between Configuration I and II. One comparison between Configuration I and III was within 1% (these are kinematically equivalent). All subsequent results were obtained with the torque transducer in Configuration III.

Friction coefficients for shaft rotation and 5 seconds of operation with 10W-40 motor oil are plotted vs. shaft speed for four loads in Figure 5. The test bearing is an unmodified Torrington B1212 full-complement 19.05 mm bore drawn cup needle bearing with 27 needle rollers. Similar data for the same bearing and cup rotation is plotted in Figure 6, along with results for a caged bearing. The caged bearing was a Torrington J1212, a 19.05 mm bore drawn cup bearing with 17 retained needles.

In all cases at lower loads the friction coefficient is sensitive to speed with values that increase with speed. At high load, the friction coefficient is reduced from that at low load and is relatively insensitive to speed. These effects can be attributed to the predominance of viscous losses at light load (speed sensitive) and Coulomb type friction at high load (speed insensitive). To check, these tests might be repeated for a low viscosity oil or a grease.

The frictional torque of the caged bearing was less than half that of the full-complement version for the same load. This can be attributed to the replacement of a roller/roller contact of infinite slide to roll ratio (for which hydrodynamic lubrication is difficult to achieve) with a cage/roller contact with slide to roll ratio of 2. The cage also guides the needles to reduce axial skew and attending friction (see later section).

The rotating cup consistently showed higher friction than the rotating shaft mode for the full-complement bearing (the caged bearing was only used in

the cup rotation mode). At low load the ratio was about 2 to 1 and for high load about 1.5 to 1. Since the affect of rotation mode is greatest at light load, viscous drag may be the cause of the difference. The rotating cup would tend to retain oil in the cup while the rotating shaft would not.

At the conclusion of the tests just discussed a new B1212 full-complement bearing was run at seven combinations of load and speed of shaft rotation to assess the effect of running in. The new bearing had an 18% on average higher frictional torque than the previous one (Figures 5 and 6) which had been used extensively for rig development testing.

A thermocouple was installed on a clamp attached to the inner spool to measure the specimen housing temperature (Figure 3). The new B1212 specimen was operated at 3000 shaft rpm and 1815 N load. The load was removed and the shaft jogged momentarily at 30, 120, 300, and 600 seconds of running to establish the zero torque level. Friction coefficient is plotted vs. housing temperature and time in Figures 7a and 7b respectively. Reference [2] presents a method for estimating friction in rolling bearings. Using typical viscosity for 10W-40 motor oil this method yields estimates of 0.0032 and 0.0016 for friction coefficients at 25 and 50°C respectively. The measured coefficients were 76% higher. The reference does not distinguish between caged and full-complement bearings in this estimate so the agreement is reasonably good.

#### Needle Angle/Thrust Tests

All results in this section are for shaft rotation in a full-complement bearing lubricated with grease. Figure 8 illustrates typical behavior when a reversal (sign change) in thrust occurs. The needle bearing appears to operate somewhat stably with a non-zero preferred thrust which will occasionally and unpredictably reverse. In fact, most attempts to record a

spontaneous thrust change on this rig were unsuccessful. Often, acceleration of the drive brought on a thrust change. This observation is in agreement with Ref [4] where it was concluded that the needles in a loaded full-complement bearing operate skewed. Note the similarity between Figures 1 and 8.

Figures 9-12 present relative needle angle, absolute thrust, relative frictional torque, and needle complement to shaft speed ratio as functions of time for two loads and three speeds. Needle angle is calculated from the phase difference between the signals from the two optical probes at needle ends (in the bearing load zone) and the average complement velocity for the entire record and the length of a needle. Needle angle is defined in Figure 4. The frictional torque which is plotted is relative since the zero torque signal level is undetermined. Also the support bearings are not jogged so that the attenuation of the signal due to support bearing friction is not known. The torque data is presented here, however, since the transients that are plotted not only show the trend of the torque response but also represent the lower limit of torque variations during a record. The needle complement speed to average shaft speed ratios plotted are for both the measured complement speed (calculated from the time required for 27 needles to pass the optical probes) and the complement speed calculated for the no slip condition from the measured shaft speed using

$$\frac{\overline{N_{compl}}}{\overline{N}_{shaft}} \Big|_{no\ slip} = \frac{r_s}{2(r_s + r_n)} \frac{N_{shaft}}{\overline{N}_{shaft}}$$

where the over-bar indicates an average over the data record and  $r_s$  and  $r_n$  are shaft and needle radii respectively. This presentation was selected because it shows the acceleration of the shaft during a record. Measured complement speed was consistently about 1.5% below the no slip speed.

It should be noted that data was only collected when a significant change in axial thrust was encountered. In Figures 9-12 there is apparently a correlation between needle angle and thrust. In Figures 10-12 there appears to be a correlation between frictional torque and needle angle. For the data of Figures 10 and 11 frictional torque and thrust were plotted as functions of needle angle in Figures 13 and 14. The record was divided into one hundred equal time intervals. Angles, torques, and thrusts were averaged over each period before being plotted. Therefore, in Figures 13 and 14 each point represents about six needle passages. The thrust vs. needle angle curve clearly shows the characteristic "S" shape of traction vs. side slip angle (Ref [6]). The traction coefficient saturates at about 0.05. Of interest also is the minimization of frictional torque at the relative needle angle for zero thrust. It can be argued that the relative angle at which thrust is zero and torque is minimized should correspond to a needle angle of zero, i.e., the needles are axially aligned. Then, for the data of Figures 13 and 14, the needle angle is equal to the relative angles less  $0.8^\circ$ . The reduction in frictional torque when the needles are axially aligned is  $0.014 \text{ N}\cdot\text{m}$  which for the load of  $860 \text{ N}$  gives a change of friction coefficient of  $\Delta\mu = 1.7 \times 10^{-3}$  or about 25% of the friction coefficient shown in Figure 5. As this  $\Delta\mu$  value has likely been attenuated by support bearing friction, the actual torque reduction may have been much greater.

In Figure 15, the angle data of Figure 10 are plotted as individual needle angles for one-fourth of the data record, centered about the middle of the record.

## Recommendations for Future Work

### Modifications to Rig

It is recommended that a fixture be developed to adjust the optical probe positions so that their respective signal waveforms are synchronized when a passing needle is parallel to the shaft axis. This would enable the determination of the true thrust at zero needle angle.

The shaft journal bearing at the left block (see Figure 2) has been shortened to accommodate shaft distortion under load and prevent seizing at high load. For extended running time another solution is needed. The shaft bearing at the right block should be made self aligning or a flexure similar to the one on the left end of the shaft should be incorporated. Either solution would allow the use of a longer journal bearing sleeve.

### Experiments

It is recommended that the following experimental programs be undertaken:

- 1) Write software and take preliminary needle angle/thrust data for the rotating cup mode.
- 2) Calculate and plot the distribution of circumferencial clearance between needles using the times of needle passages with the assumption of constant complement speed.
- 3) Measure frictional torque for various viscosities and volumes of liquid lubricant.
- 4) Measure needle angle and thrust for a caged bearing. A special cage might be required.

- 5) Measure needle/cage forces using the defection of a cage element which can be detected by the existing optical probes viewing targets on the cage.\*<sup>1</sup>

In many full-complement needle bearing applications a means of reacting the thrust generated by the needle bearing must be provided , e.g., thrust bearing surfaces on the faces of transmission planet gears. If a geometry (needle aspect ratio, clearance, etc.) can be found which minimizes needle skew and thereby thrust, this requirement may be relaxed and limiting speed would probably be higher. Frictional torque would be reduced. All of which would increase the applications for these full-complement bearings.

#### References

1. Tedric A. Harris, Rolling Bearing Analysis, John Wiley and Sons, 1984, p. 425-427.
2. Eschmann, Hasbargen, Weigand, Ball and Roller Bearings, John Wiley and Sons, 1985.
3. L. J. Nypan, "Roller Skewing Behavior in Roller Bearings," ASME, JOLT, Vol. 104, July 1982.
4. Ulezelski, Evans, Haka, Malloy, "Needle Bearing Axial Thrust Study," Society of Automotive Engineers, 830568, 1983.
5. Bair, Winer and Griffioen, "The Tribological Behavior of an Automotive Cam and Lifter System," Trans. ASME, JOT, 108, 1986.
6. Johnson, K. L., and Tevaarwerk, J. L., "Shear Behavior of Elastohydrodynamic Oil Films," Proc. Roy Soc. of London, 365A, 1977.

---

<sup>1</sup>\*\*Requires a special cage with an element which deflects under the force of needle contact and multiplies this defection to a detectable level of about 0.05 mm.



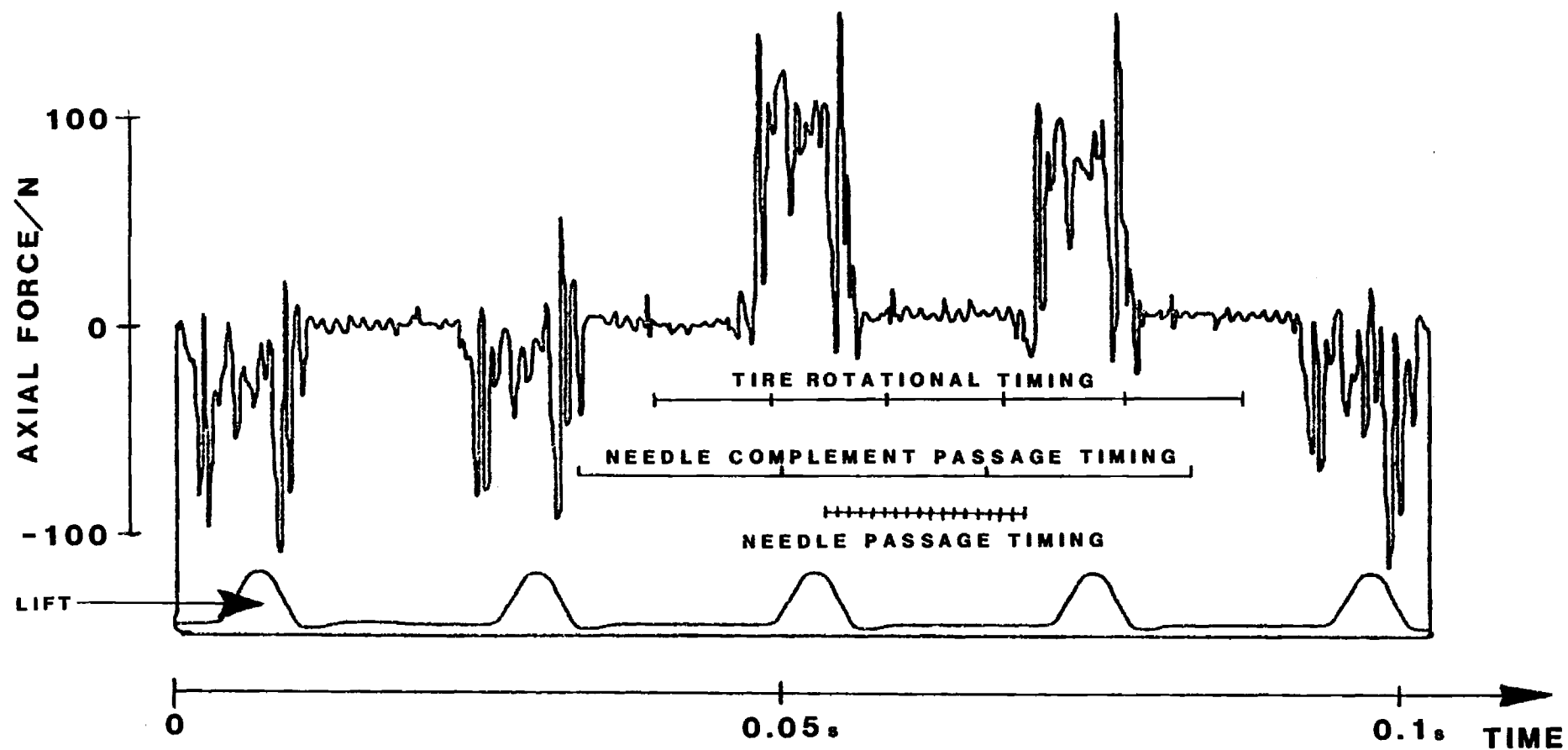


Figure 1. Shaft Axial Force for a Needle Roller  
Tappet at 2700 rpm of cam

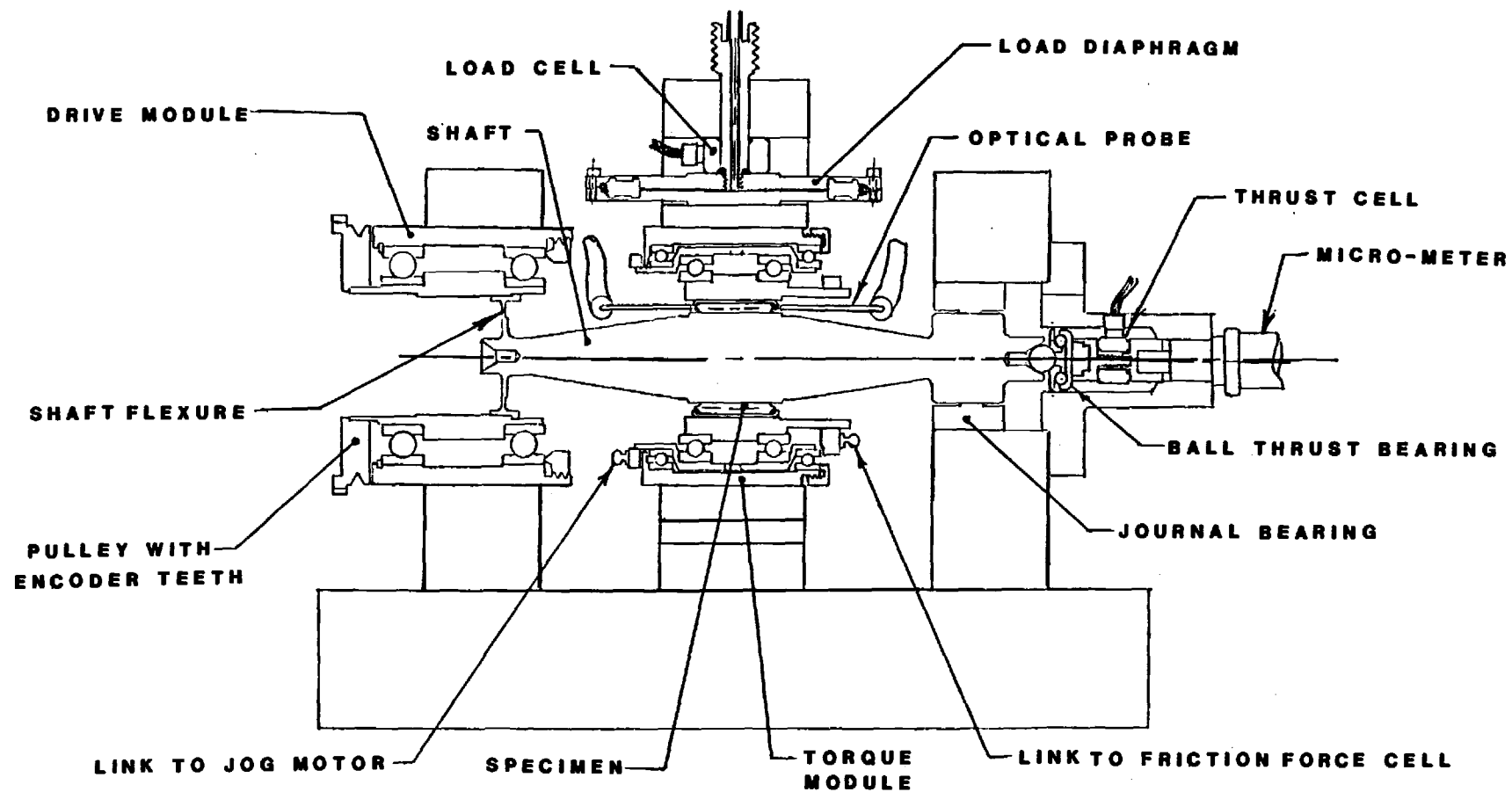
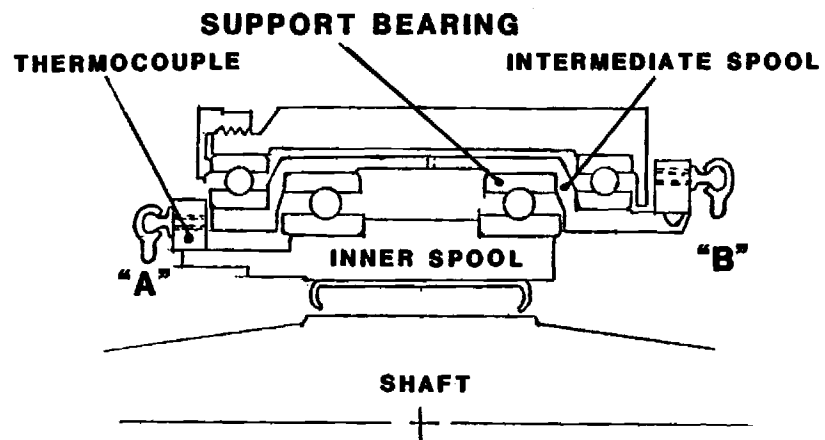
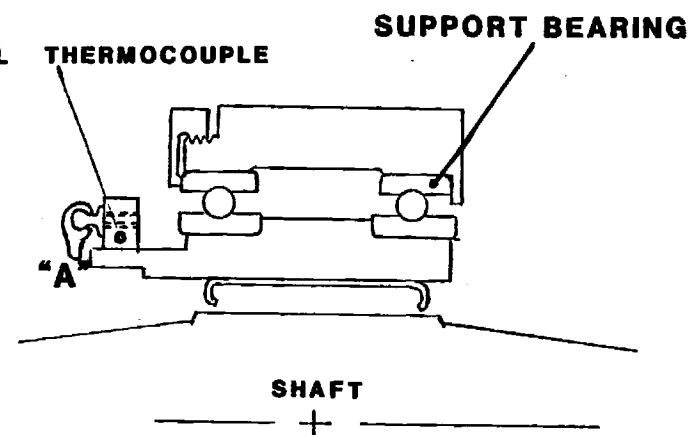


Figure 2. Needle Bearing Simulator

### FOUR-BEARING TORQUE MODULE



### TWO-BEARING TORQUE MODULE



### CONFIGURATIONS

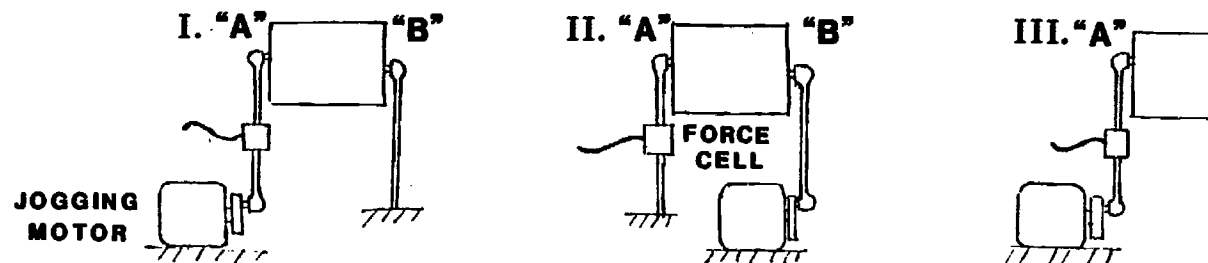


Figure 3. Torque Transducer Configurations

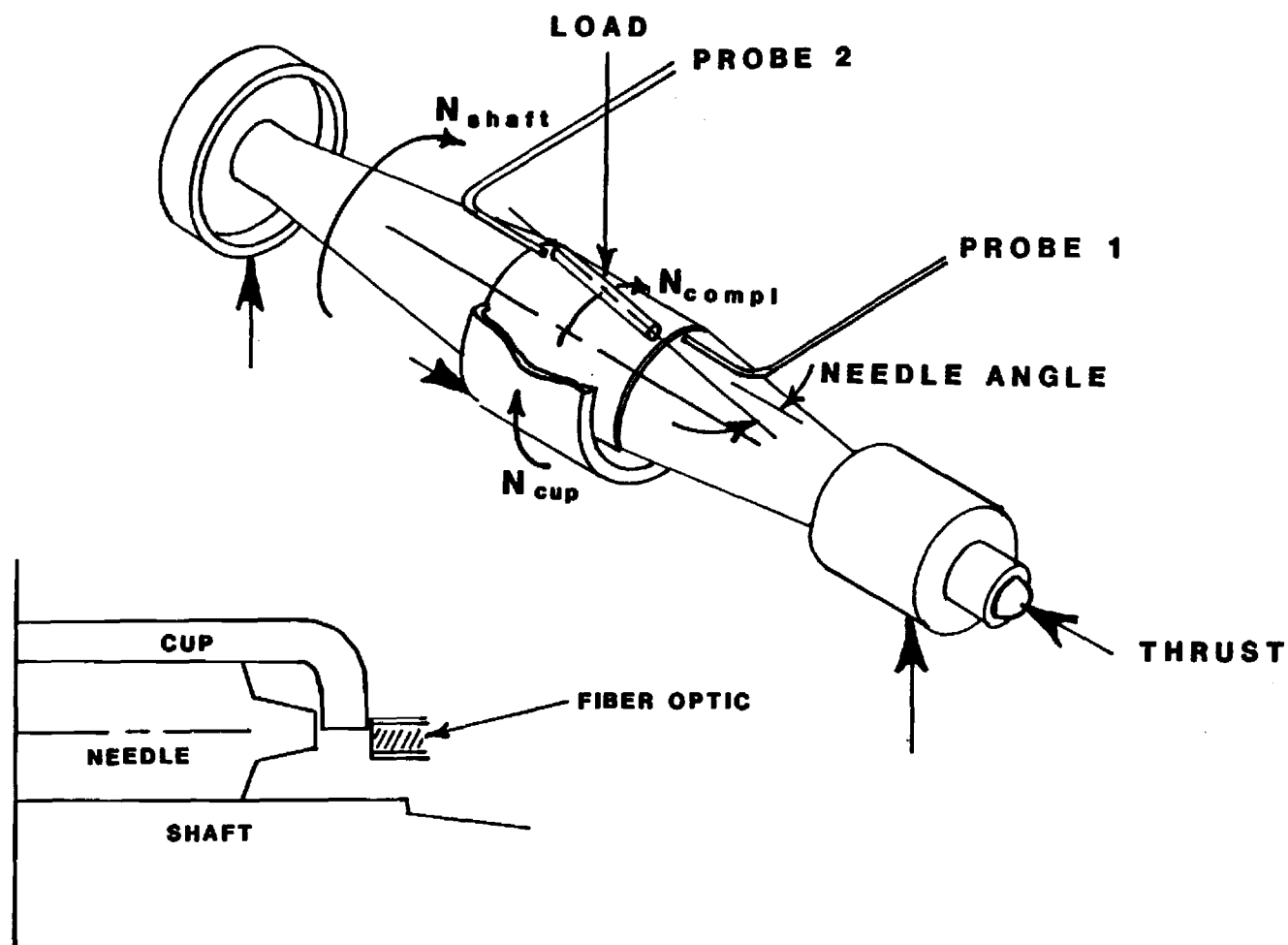


Figure 4. Definitions of Rotation Directions, Load, Thrust and Needle Angle and Optical Probe Detail

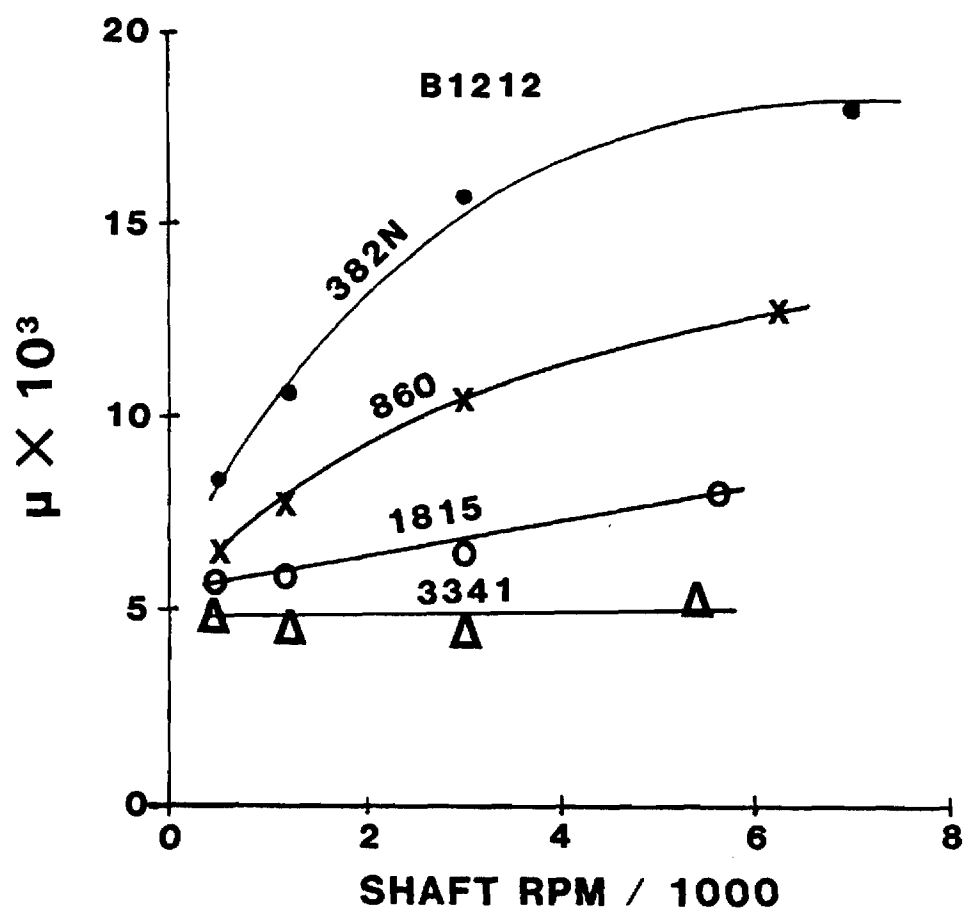


Figure 5. Friction Coefficient,  $\mu$ , for shaft rotation, 5 sec running, Configuration III, 10W-40 motor oil

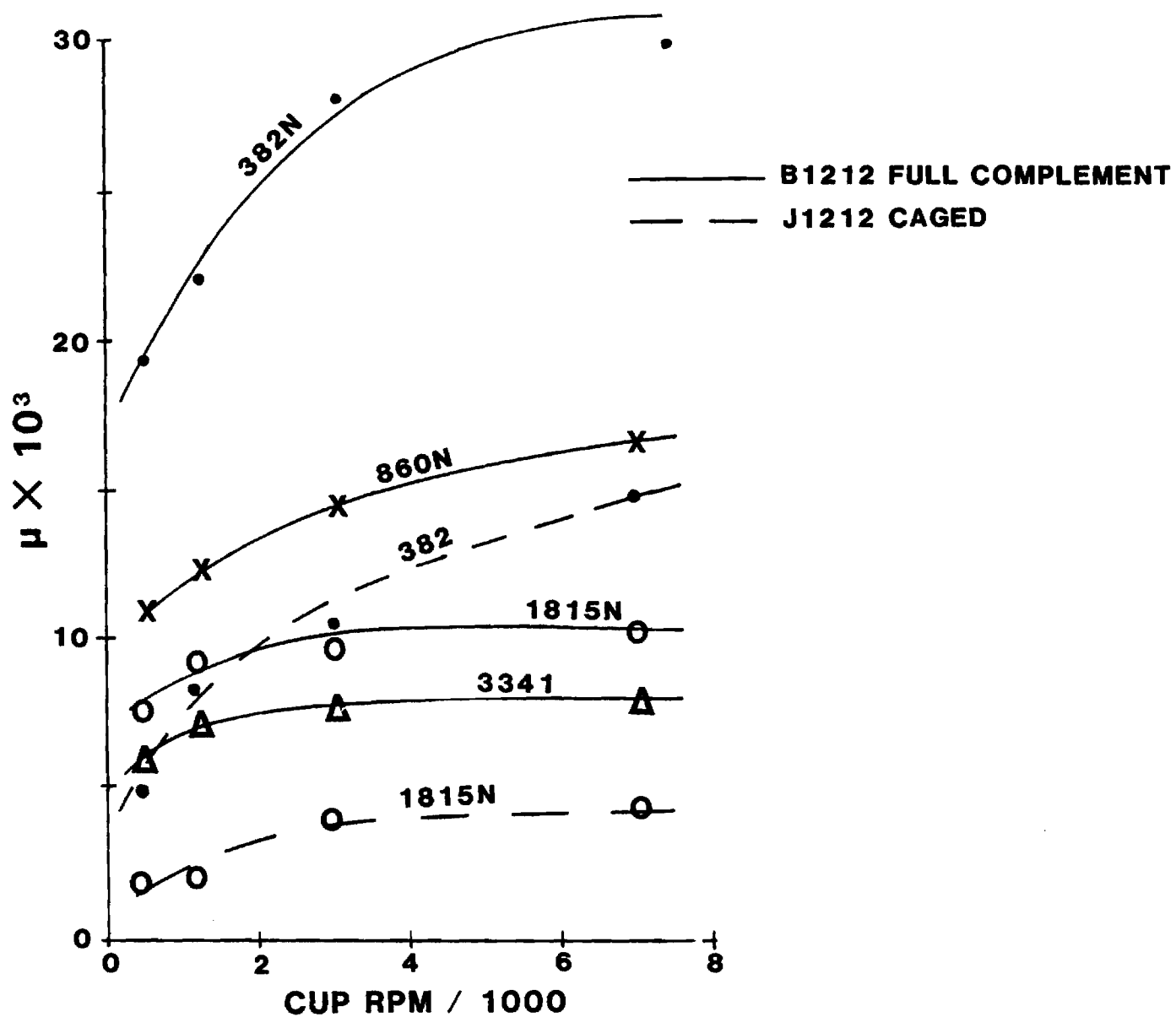


Figure 6. Friction Coefficient,  $\mu$ , for cup rotation, 5 sec running, Configuration III, 10W-40 motor oil

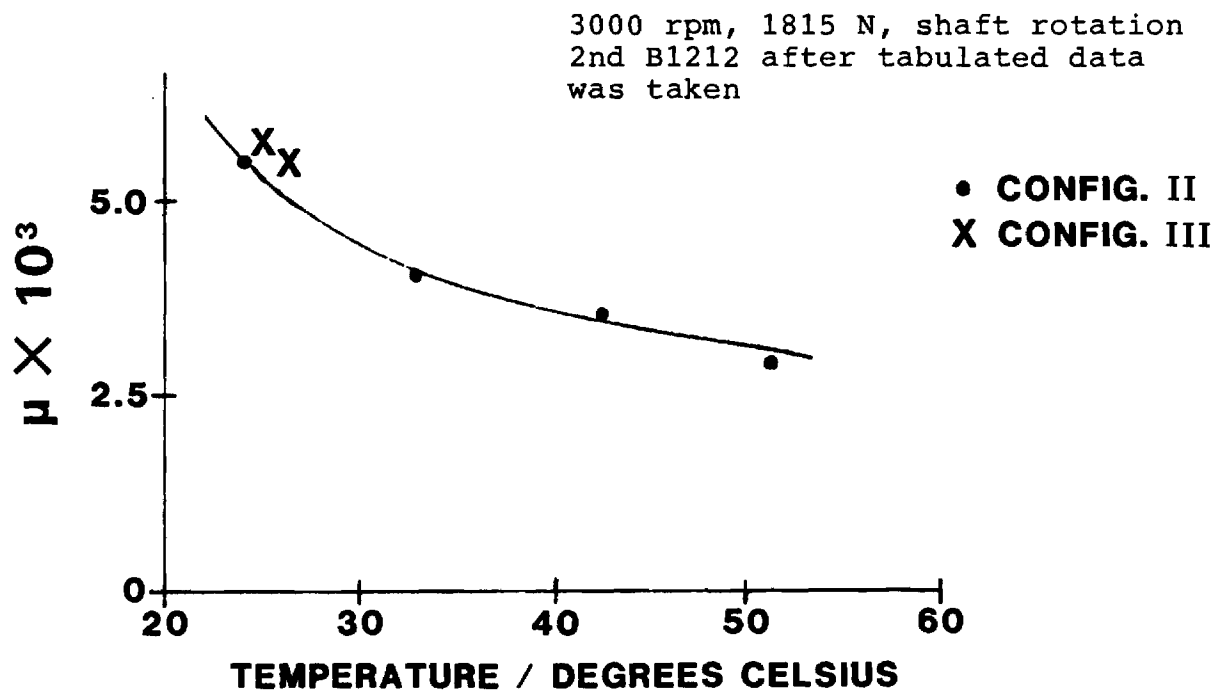


Figure 7a. Friction coefficient vs. temperature of housing edge. Thermocouple shown in Figure 1

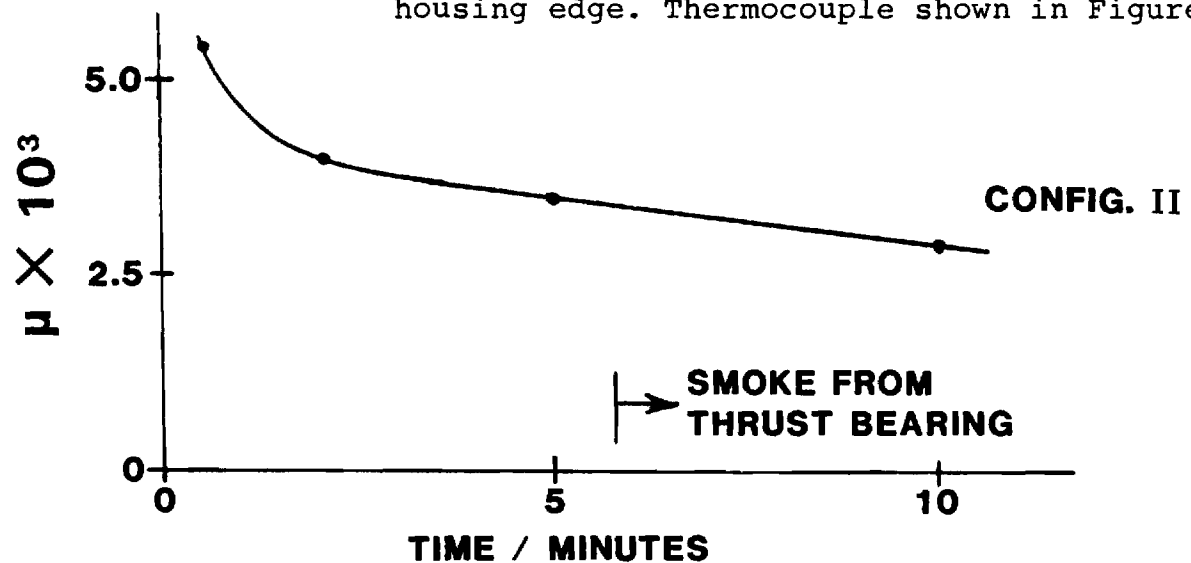


Figure 7b. Data of 7a. plotted for running time

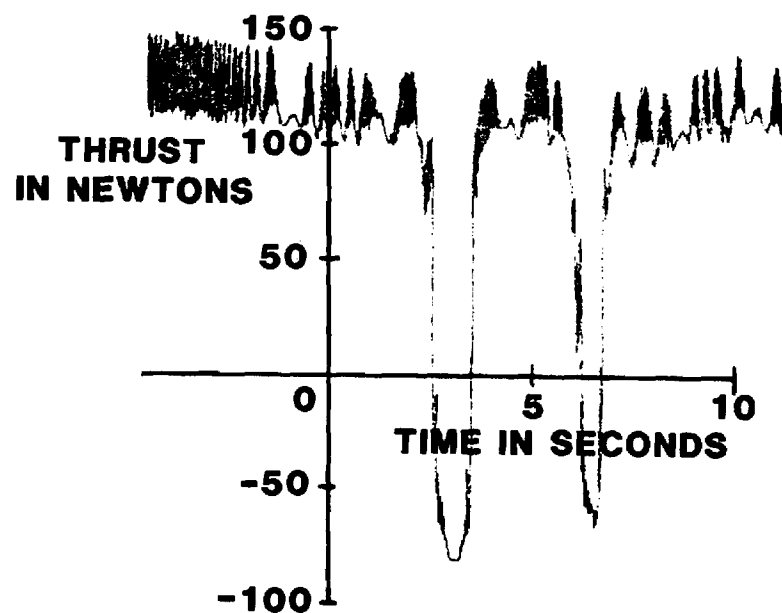


Figure 8. Axial Thrust for B1212 at 3000 rpm of Shaft and 1815 N Load, Oil Lubricated.



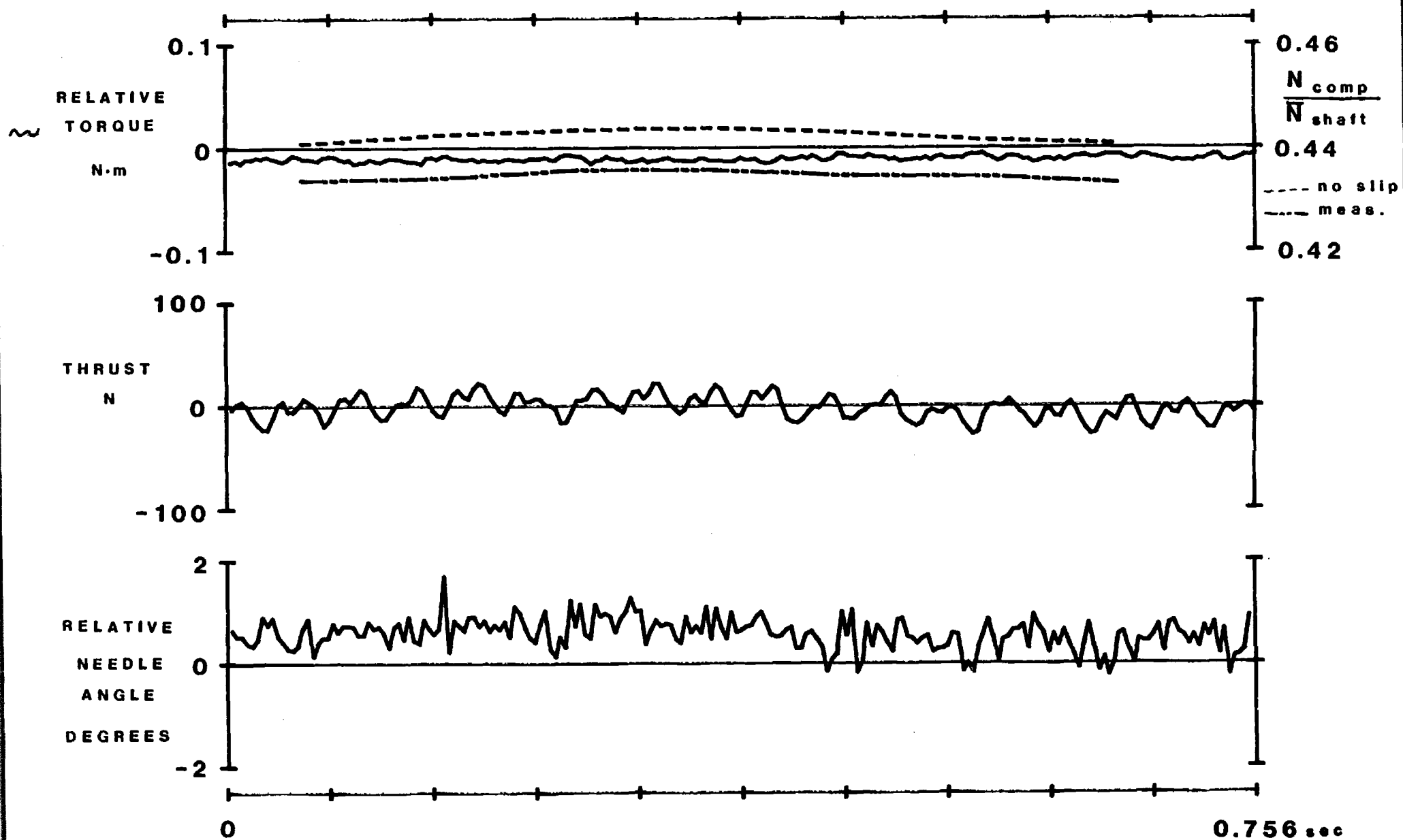


Figure 9. Run C, 382 N load,  $\bar{N}_{shaft} = 1381$  rpm, grease

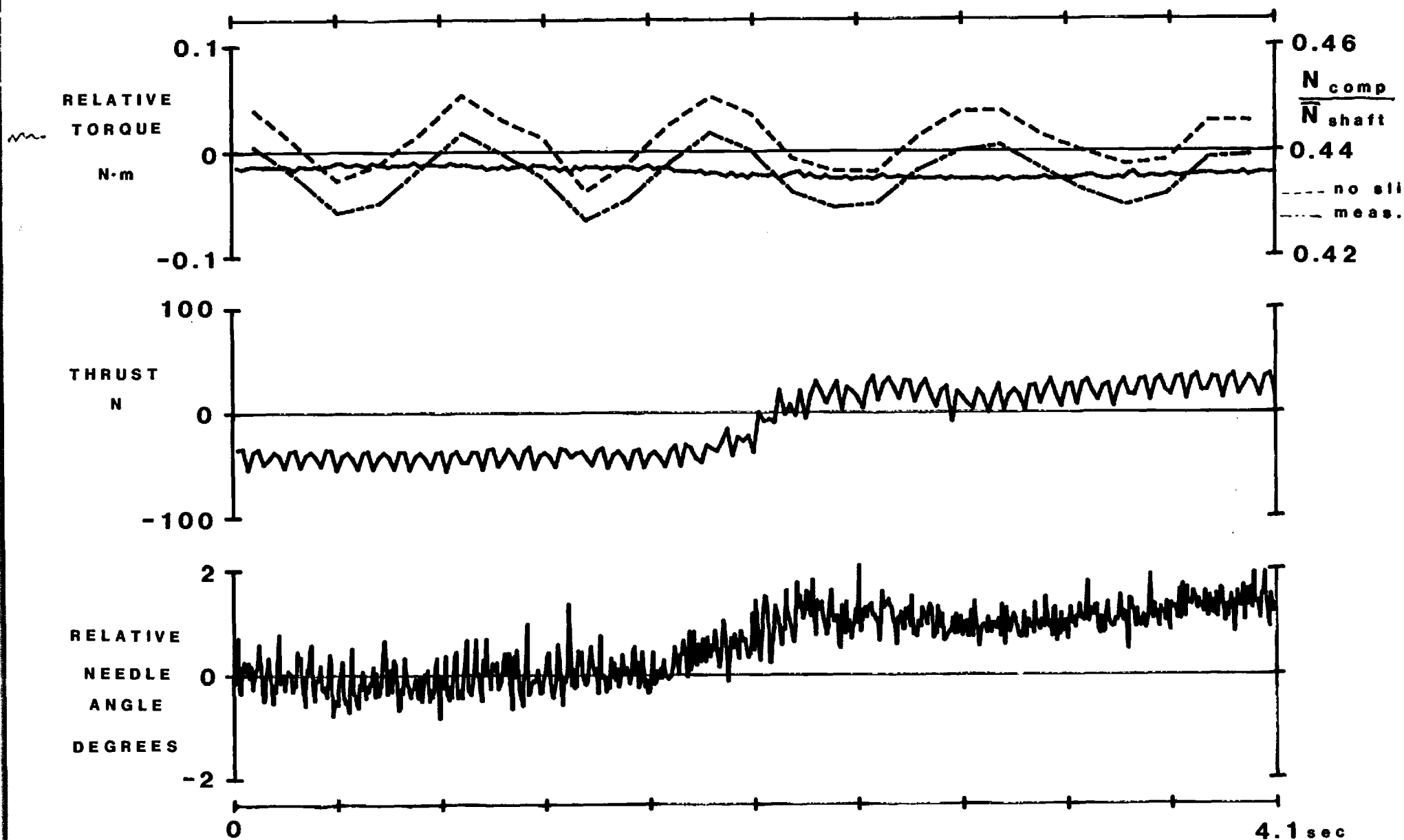


Figure 10. Run D,  $\bar{N}_{shaft} = 841$  rpm, 860 N load, grease

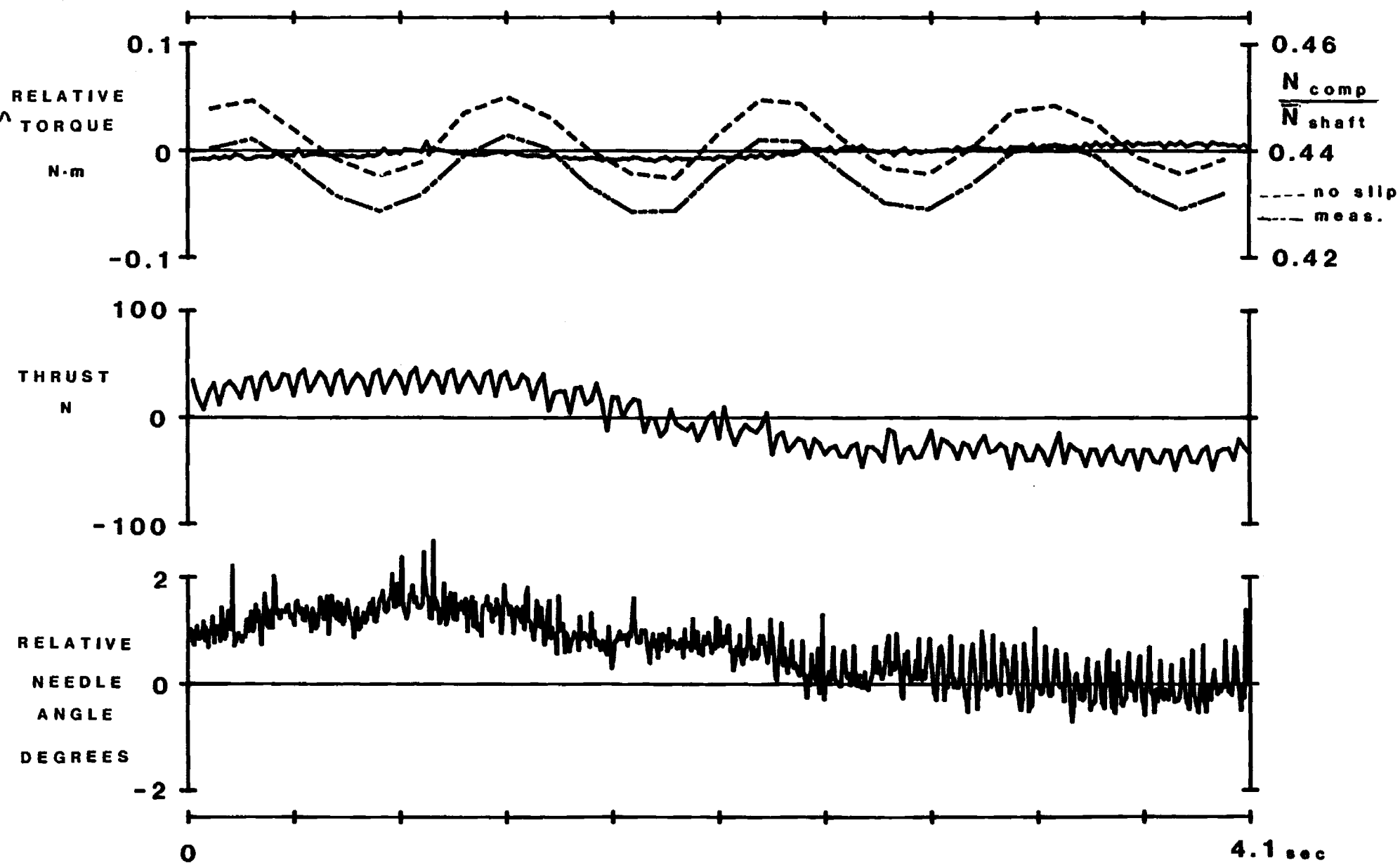


Figure 11. Run E,  $\bar{N}_{shaft} = 850$  rpm, 860 N load, grease

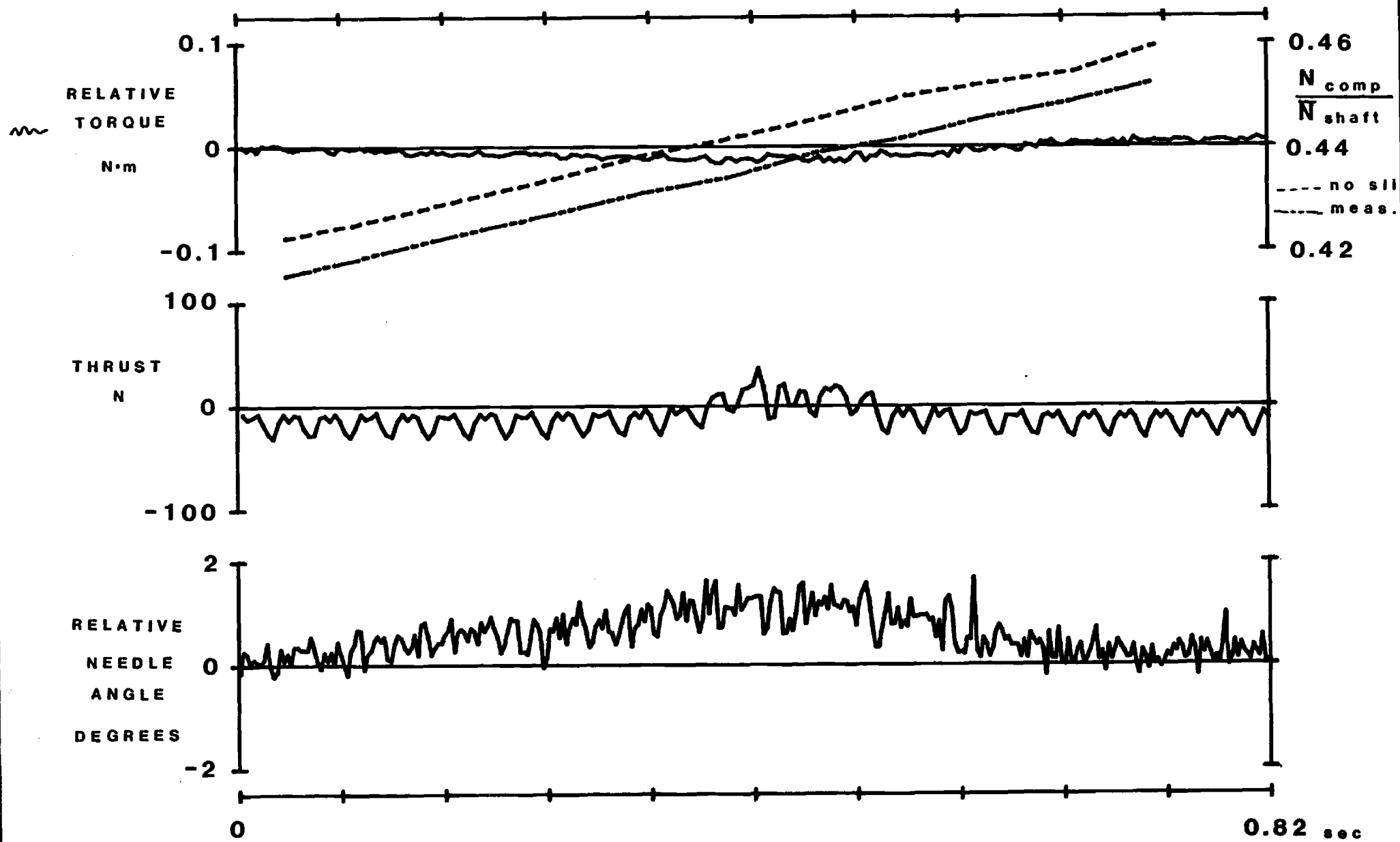


Figure 12. Run G,  $\bar{N}_{shaft} = 2000$  rpm, 382 N load, grease

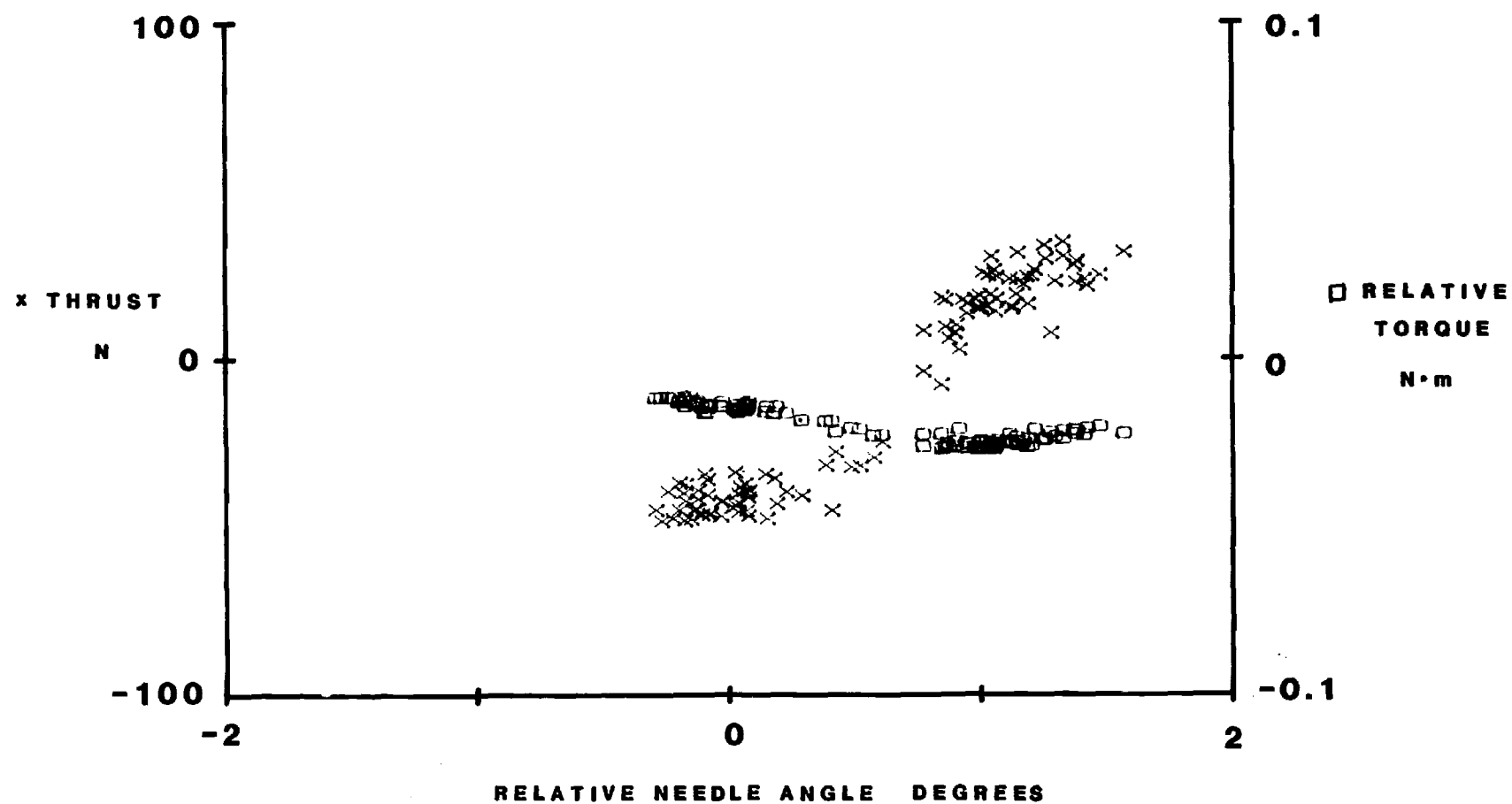


Figure 13. Run D,  $\bar{N}_{\text{shaft}} = 841$  rpm, 860 N load, grease

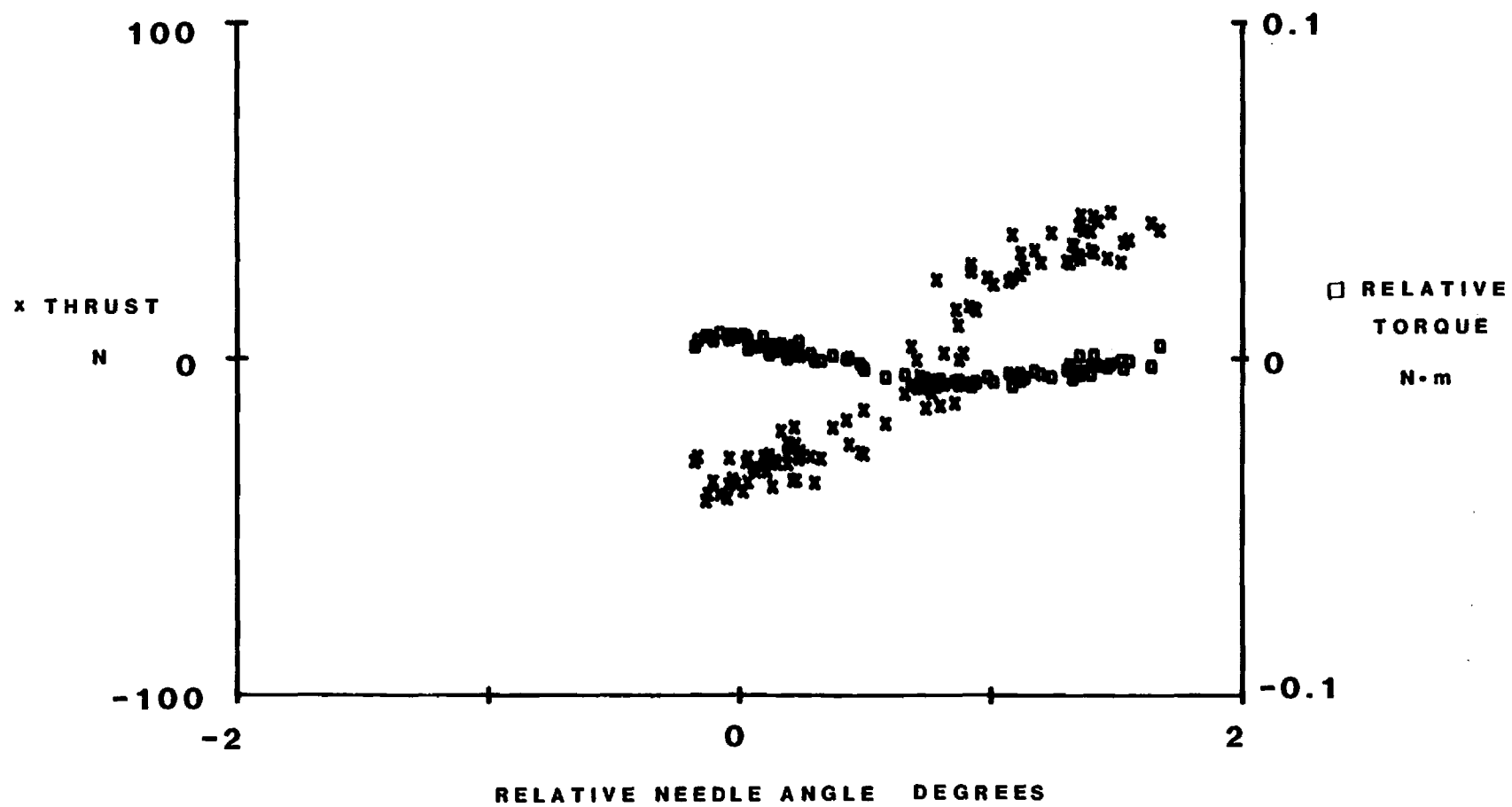


Figure 14. Run E,  $\bar{N}_{\text{shaft}} = 850$  rpm, 860 N load, grease

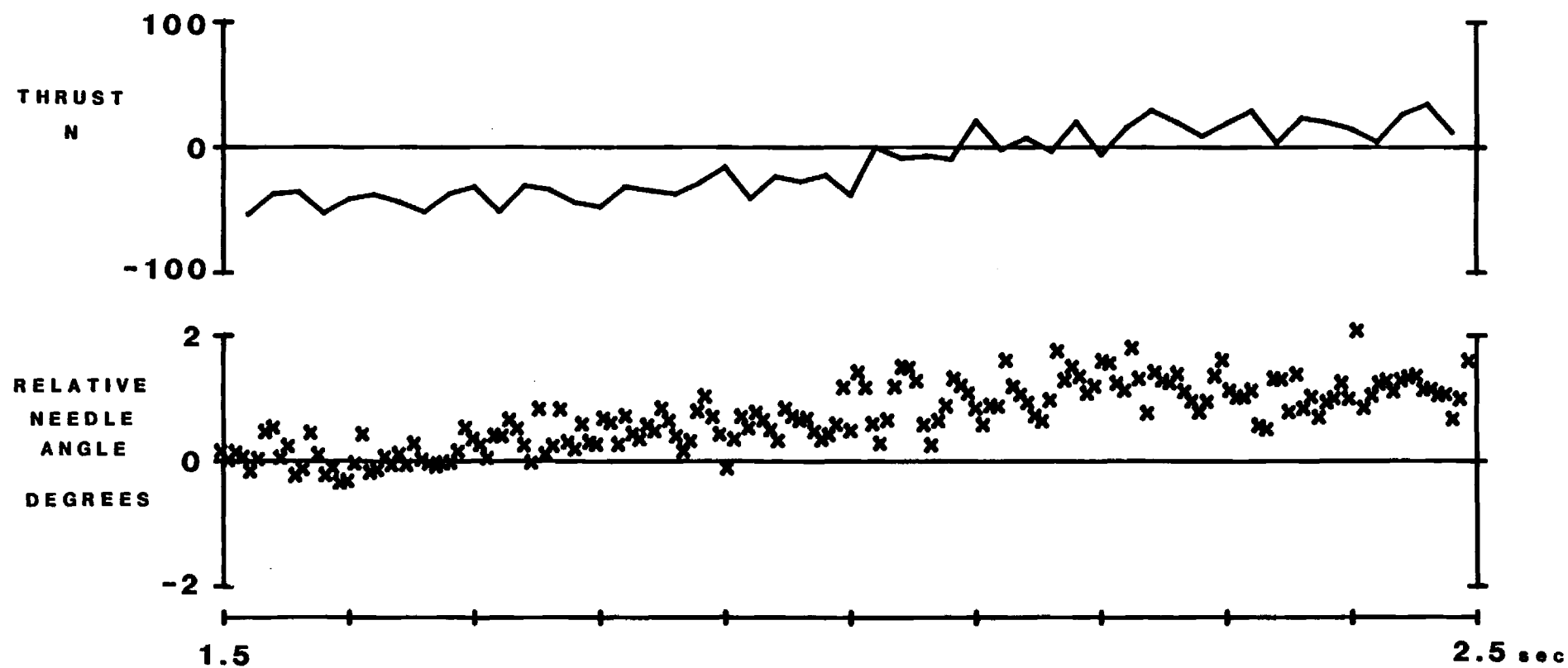


Figure 15. Run D,  $\bar{N}_{\text{shaft}} = 841 \text{ rpm}$ , 860 N - Individual Needle Angles and Corresponding Thrust